Frontiers of Information Technology & Electronic Engineering
www.jzus.zju.edu.cn; engineering.cae.cn; www.springerlink.com
ISSN 2095-9184 (print); ISSN 2095-9230 (online)
E-mail: jzus@zju.edu.cn

Supplementary materials for

Zelong CUI, Jun LIU, Gang YANG, 2024. XL-RIS empowered near-field physical layer security against jamming and eavesdropping attacks. *Front Inform Technol Electron Eng*, 25(12):1750-1758.
https://doi.org/10.1631/FITEE.2400477

1 Supplement to notations and formula definitions

1.1 Notations

The main notations are presented as follows: $\mathcal{CN}\left(\mu,\sigma^2\right)$ denotes the circularly symmetric complex Gaussian distribution with mean μ and variance σ^2. For any vector $\boldsymbol{v}$, v_i denotes the i^{th} element, $\left\|\boldsymbol{v}\right\|$ denotes the Euclidean norm, and diag($\boldsymbol{v}$) denotes the diagonal operation. For any matrix $\boldsymbol{V}$, $V_{i,j}$ is the i^{th} row and j^{th} column element, and the transpose and conjugate transpose are $\boldsymbol{V}^{\mathrm{T}}$ and $\boldsymbol{V}^{\mathrm{H}}$, respectively. $\left|x\right|$ denotes the absolute value of x, and $\mathrm{Re}\{x\}$ is its real part. $\otimes$ denotes the Kronecker product.

1.2 Formula definitions in Sections 3.1 and 3.2

$\boldsymbol{A}_{\mathrm{U}}$, $\boldsymbol{A}_{\mathrm{E}}$, and c_{U1} in Section 3.1 are defined as Eq. (S1):

$$\begin{aligned}
\boldsymbol{A}_{\mathrm{U}} &= \left(\boldsymbol{\theta}^{\mathrm{H}}\mathrm{diag}\left(\mathbf{h}_{\mathrm{RU}}^{\mathrm{H}}\right)\mathbf{H}_{\mathrm{SR}}+\mathbf{h}_{\mathrm{SU}}^{\mathrm{H}}\right)^{\mathrm{H}}\left(\boldsymbol{\theta}^{\mathrm{H}}\mathrm{diag}\left(\mathbf{h}_{\mathrm{RU}}^{\mathrm{H}}\right)\mathbf{H}_{\mathrm{SR}}+\mathbf{h}_{\mathrm{SU}}^{\mathrm{H}}\right),\\
\boldsymbol{A}_{\mathrm{E}} &= \left(\boldsymbol{\theta}^{\mathrm{H}}\mathrm{diag}\left(\mathbf{h}_{\mathrm{RE}}^{\mathrm{H}}\right)\mathbf{H}_{\mathrm{SR}}+\mathbf{h}_{\mathrm{SE}}^{\mathrm{H}}\right)^{\mathrm{H}}\left(\boldsymbol{\theta}^{\mathrm{H}}\mathrm{diag}\left(\mathbf{h}_{\mathrm{RE}}^{\mathrm{H}}\right)\mathbf{H}_{\mathrm{SR}}+\mathbf{h}_{\mathrm{SE}}^{\mathrm{H}}\right),\\
c_{\mathrm{U1}} &= \left|\left(\boldsymbol{\theta}^{\mathrm{H}}\mathrm{diag}\left(\mathbf{h}_{\mathrm{RU}}^{\mathrm{H}}\right)\mathbf{H}_{\mathrm{JR}}+\mathbf{h}_{\mathrm{JU}}^{\mathrm{H}}\right)\boldsymbol{m}\right|^2+\sigma_{\mathrm{u}}^2.
\end{aligned} \tag{S1}$$

The formula manipulation in Section 3.2 can be introduced to obtain $\boldsymbol{G}_{\mathrm{u},1}$, $b_{\mathrm{u},1}$, $\boldsymbol{G}_{\mathrm{u},2}$, $b_{\mathrm{u},2}$, $\boldsymbol{G}_{\mathrm{e},1}$, $b_{\mathrm{e},1}$, $\boldsymbol{G}_{\mathrm{e},2}$, $b_{\mathrm{e},2}$, $\boldsymbol{G}_{\mathrm{j}}$, and b_{j} as the following Eq. (S2):

$$\begin{aligned}
\boldsymbol{G}_{\mathrm{u},1} &= \begin{bmatrix}\mathrm{diag}\left(\mathbf{h}_{\mathrm{RU}}^{\mathrm{H}}\right)\mathbf{H}_{\mathrm{SR}}\boldsymbol{w}\boldsymbol{w}^{\mathrm{H}}\mathbf{H}_{\mathrm{SR}}^{\mathrm{H}}\mathrm{diag}\left(\mathbf{h}_{\mathrm{RU}}\right) & \mathrm{diag}\left(\mathbf{h}_{\mathrm{RU}}^{\mathrm{H}}\right)\mathbf{H}_{\mathrm{SR}}\boldsymbol{w}\boldsymbol{w}^{\mathrm{H}}\mathbf{h}_{\mathrm{SU}}\\ \mathbf{h}_{\mathrm{SU}}^{\mathrm{H}}\boldsymbol{w}\boldsymbol{w}^{\mathrm{H}}\mathbf{H}_{\mathrm{SR}}^{\mathrm{H}}\mathrm{diag}\left(\mathbf{h}_{\mathrm{RU}}\right) & 0\end{bmatrix}, b_{\mathrm{u},1}=\mathbf{h}_{\mathrm{SU}}^{\mathrm{H}}\boldsymbol{w}\boldsymbol{w}^{\mathrm{H}}\mathbf{h}_{\mathrm{SU}},\\
\boldsymbol{G}_{\mathrm{u},2} &= \begin{bmatrix}\mathrm{diag}\left(\mathbf{h}_{\mathrm{RU}}^{\mathrm{H}}\right)\mathbf{H}_{\mathrm{SR}}\boldsymbol{v}\boldsymbol{v}^{\mathrm{H}}\mathbf{H}_{\mathrm{SR}}^{\mathrm{H}}\mathrm{diag}\left(\mathbf{h}_{\mathrm{RU}}\right) & \mathrm{diag}\left(\mathbf{h}_{\mathrm{RU}}^{\mathrm{H}}\right)\mathbf{H}_{\mathrm{SR}}\boldsymbol{v}\boldsymbol{v}^{\mathrm{H}}\mathbf{h}_{\mathrm{SU}}\\ \mathbf{h}_{\mathrm{SU}}^{\mathrm{H}}\boldsymbol{v}\boldsymbol{v}^{\mathrm{H}}\mathbf{H}_{\mathrm{SR}}^{\mathrm{H}}\mathrm{diag}\left(\mathbf{h}_{\mathrm{RU}}\right) & 0\end{bmatrix}, b_{\mathrm{u},2}=\mathbf{h}_{\mathrm{SU}}^{H}\boldsymbol{v}\boldsymbol{v}^{H}\mathbf{h}_{\mathrm{SU}},\\
\boldsymbol{G}_{\mathrm{e},1} &= \begin{bmatrix}\mathrm{diag}\left(\mathbf{h}_{\mathrm{RE}}^{\mathrm{H}}\right)\mathbf{H}_{\mathrm{SR}}\boldsymbol{w}\boldsymbol{w}^{\mathrm{H}}\mathbf{H}_{\mathrm{SR}}^{\mathrm{H}}\mathrm{diag}\left(\mathbf{h}_{\mathrm{RE}}\right) & \mathrm{diag}\left(\mathbf{h}_{\mathrm{RE}}^{\mathrm{H}}\right)\mathbf{H}_{\mathrm{SR}}\boldsymbol{w}\boldsymbol{w}^{\mathrm{H}}\mathbf{h}_{\mathrm{SE}}\\ \mathbf{h}_{\mathrm{SE}}^{\mathrm{H}}\boldsymbol{w}\boldsymbol{w}^{\mathrm{H}}\mathbf{H}_{\mathrm{SR}}^{\mathrm{H}}\mathrm{diag}\left(\mathbf{h}_{\mathrm{RE}}\right) & 0\end{bmatrix}, b_{\mathrm{e},1}=\mathbf{h}_{\mathrm{SE}}^{H}\boldsymbol{w}\boldsymbol{w}^{H}\mathbf{h}_{\mathrm{SE}},\\
\boldsymbol{G}_{\mathrm{e},2} &= \begin{bmatrix}\mathrm{diag}\left(\mathbf{h}_{\mathrm{RE}}^{\mathrm{H}}\right)\mathbf{H}_{\mathrm{SR}}\boldsymbol{v}\boldsymbol{v}^{\mathrm{H}}\mathbf{H}_{\mathrm{SR}}^{\mathrm{H}}\mathrm{diag}\left(\mathbf{h}_{\mathrm{RE}}\right) & \mathrm{diag}\left(\mathbf{h}_{\mathrm{RE}}^{\mathrm{H}}\right)\mathbf{H}_{\mathrm{SR}}\boldsymbol{v}\boldsymbol{v}^{\mathrm{H}}\mathbf{h}_{\mathrm{SE}}\\ \mathbf{h}_{\mathrm{SE}}^{\mathrm{H}}\boldsymbol{v}\boldsymbol{v}^{\mathrm{H}}\mathbf{H}_{\mathrm{SR}}^{\mathrm{H}}\mathrm{diag}\left(\mathbf{h}_{\mathrm{RE}}\right) & 0\end{bmatrix}, b_{\mathrm{e},2}=\mathbf{h}_{\mathrm{SE}}^{\mathrm{H}}\boldsymbol{v}\boldsymbol{v}^{\mathrm{H}}\mathbf{h}_{\mathrm{SE}},\\
\boldsymbol{G}_{\mathrm{j}} &= \begin{bmatrix}\mathrm{diag}\left(\mathbf{h}_{\mathrm{RU}}^{\mathrm{H}}\right)\mathbf{H}_{\mathrm{JR}}\boldsymbol{m}\boldsymbol{m}^{\mathrm{H}}\mathbf{H}_{\mathrm{JR}}^{\mathrm{H}}\mathrm{diag}\left(\mathbf{h}_{\mathrm{RU}}\right) & \mathrm{diag}\left(\mathbf{h}_{\mathrm{RU}}^{\mathrm{H}}\right)\mathbf{H}_{\mathrm{JR}}\boldsymbol{m}\boldsymbol{m}^{\mathrm{H}}\mathbf{h}_{\mathrm{JU}}\\ \mathbf{h}_{\mathrm{JU}}^{\mathrm{H}}\boldsymbol{m}\boldsymbol{m}^{\mathrm{H}}\mathbf{H}_{\mathrm{JR}}^{\mathrm{H}}\mathrm{diag}\left(\mathbf{h}_{\mathrm{RU}}\right) & 0\end{bmatrix}, b_{\mathrm{j}}=\mathbf{h}_{\mathrm{JU}}^{\mathrm{H}}\boldsymbol{m}\boldsymbol{m}^{\mathrm{H}}\mathbf{h}_{\mathrm{JU}}.
\end{aligned} \tag{S2}$$

Manifold optimization (MO) is divided mainly into the following three steps:

1. Computation of Riemannian gradient: With the reformulation, the Euclidean gradient of C_{S} can be easily obtained. We use ∇f to represent the Euclidean gradient of C_{S}, which can be expressed as Eq. (S3). Then, the Riemannian gradient $\mathrm{grad}f$ can be expressed as Eq. (S4).

$$\nabla f = \frac{1}{\ln 2}\left(\frac{2\boldsymbol{G}_{\mathrm{u},1}\boldsymbol{s} + 2\boldsymbol{G}_{\mathrm{u},2}\boldsymbol{s} + 2\boldsymbol{G}_{\mathrm{j}}\boldsymbol{s}}{\boldsymbol{s}^{\mathrm{H}}\boldsymbol{G}_{\mathrm{u},1}\boldsymbol{s} + \boldsymbol{s}^{\mathrm{H}}\boldsymbol{G}_{\mathrm{u},2}\boldsymbol{s} + \boldsymbol{s}^{\mathrm{H}}\boldsymbol{G}_{\mathrm{j}}\boldsymbol{s} + b_{\mathrm{j}} + b_{\mathrm{u},1} + b_{\mathrm{u},2} + \sigma_{\mathrm{u}}^2} - \frac{2\boldsymbol{G}_{\mathrm{u},2}\boldsymbol{s} + 2\boldsymbol{G}_{\mathrm{j}}\boldsymbol{s}}{\boldsymbol{s}^{\mathrm{H}}\boldsymbol{G}_{\mathrm{u},2}\boldsymbol{s} + \boldsymbol{s}^{\mathrm{H}}\boldsymbol{G}_{\mathrm{j}}\boldsymbol{s} + b_{\mathrm{j}} + b_{\mathrm{u},2} + \sigma_{\mathrm{u}}^2} + \frac{2\boldsymbol{G}_{\mathrm{e},2}\boldsymbol{s}}{\boldsymbol{s}^{\mathrm{H}}\boldsymbol{G}_{\mathrm{e},2}\boldsymbol{s} + b_{\mathrm{e},2} + \sigma_{\mathrm{e}}^2} - \frac{2\boldsymbol{G}_{\mathrm{e},1}\boldsymbol{s} + 2\boldsymbol{G}_{\mathrm{e},2}\boldsymbol{s}}{\boldsymbol{s}^{\mathrm{H}}\boldsymbol{G}_{\mathrm{e},1}\boldsymbol{s} + \boldsymbol{s}^{\mathrm{H}}\boldsymbol{G}_{\mathrm{e},2}\boldsymbol{s} + b_{\mathrm{e},1} + b_{\mathrm{e},2} + \sigma_{\mathrm{e}}^2} \right). \tag{S3}$$

$$\mathrm{grad}f = \nabla f - \mathrm{Re}\left\{\nabla f \circ \boldsymbol{s}^*\right\} \circ \boldsymbol{s}. \tag{S4}$$

2. Finding search direction: The search direction $\boldsymbol{d}$ is selected as the tangent vector conjugate to $\mathrm{grad}f$, which can be expressed as follows:

$$\boldsymbol{d} = -\mathrm{grad}f + \tau_1 T(\bar{\boldsymbol{d}}), \tag{S5}$$

where τ_1 is the conjugate gradient update parameter, $\bar{\mathbf{d}}$ is the previous search direction, and $T(\mathbf{d})$ is the vector transport function given by

$$T(\boldsymbol{d}) = \bar{\boldsymbol{d}} - \mathrm{Re}\left\{\boldsymbol{d} \circ \boldsymbol{s}^*\right\} \circ \boldsymbol{s}. \tag{S6}$$

3. Retraction: After obtaining the optimization solution, the tangent vector should be projected back to the complex circle manifold, i.e.,

$$\boldsymbol{s}_n \leftarrow \frac{(\boldsymbol{s} + \tau_2 \boldsymbol{d})_n}{|(\boldsymbol{s} + \tau_2 \boldsymbol{d})_n|}, \forall n = 1, \ldots, N+1, \tag{S7}$$

where $\boldsymbol{s}$ is the solution in the last iteration, and τ_2 is the step size updated by the Armijo rule generally. Furthermore, we introduce $\boldsymbol{\theta} = \frac{\boldsymbol{s}_{(1:N)}}{\boldsymbol{s}_{N+1}}$ to recover $\boldsymbol{\theta}$.

2 Supplement to convergence, complexity, and additional result analysis

2.1 Convergence and complexity analysis

The overall algorithm is summarized as Algorithm 1. The number of iterations for Algorithm 1 is denoted by t. Since both the successive convex approximation (SCA) based and MO-based algorithms are guaranteed to converge, the objective value satisfies the following inequality:

$$C_{\mathrm{S}}\left(\boldsymbol{w}^{(n)}, \boldsymbol{v}^{(n)}, \boldsymbol{\Theta}^{(n)}\right) \le C_{\mathrm{S}}\left(\boldsymbol{w}^{(n+1)}, \boldsymbol{v}^{(n+1)}, \boldsymbol{\Theta}^{(n)}\right) \le C_{\mathrm{S}}\left(\boldsymbol{w}^{(n+1)}, \boldsymbol{v}^{(n+1)}, \boldsymbol{\Theta}^{(n+1)}\right). \tag{S8}$$

The above inequality implies that the objective value sequence $\left\{C_{\mathrm{S}}\left(\boldsymbol{w}^{(n)}\boldsymbol{v}^{(n)}, \boldsymbol{\Theta}^{(n)}\right), t = 1, 2, \ldots\right\}$ increases monotonically. Since there exists an upper bound for the secrecy capacity due to the limited transmit power at the base station, Algorithm 1 is guaranteed to converge.

The computational complexity for the MO-based algorithm is given by $\mathcal{O}\left(N^2\right)$ (Guo HY et al., 2020), and the computational complexity for solving problem (18) is given by $\mathcal{O}\left(M^3\right)$ (Ben-Tal and Nemirovski, 2001).

Hence, the total computational complexity of Algorithm 1 is $\mathcal{O}\left(t\left(N^2+M^3\right)\right)$.

2.2 Additional result analysis

Fig. S1 shows the secrecy capacity versus the transmit power P_{J} for different baseline schemes. Set $N_{\mathrm{H}}=100$, $M=8$, and $P=40$ dBm. It can be observed that as the transmit power of the jammer increases, the secrecy capacity of all the schemes decreases. When $P_{\mathrm{J}}=20$ dBm, the secrecy capacity of the proposed algorithm increases by 31.3% and 67.0% compared with that of the two other schemes, respectively.

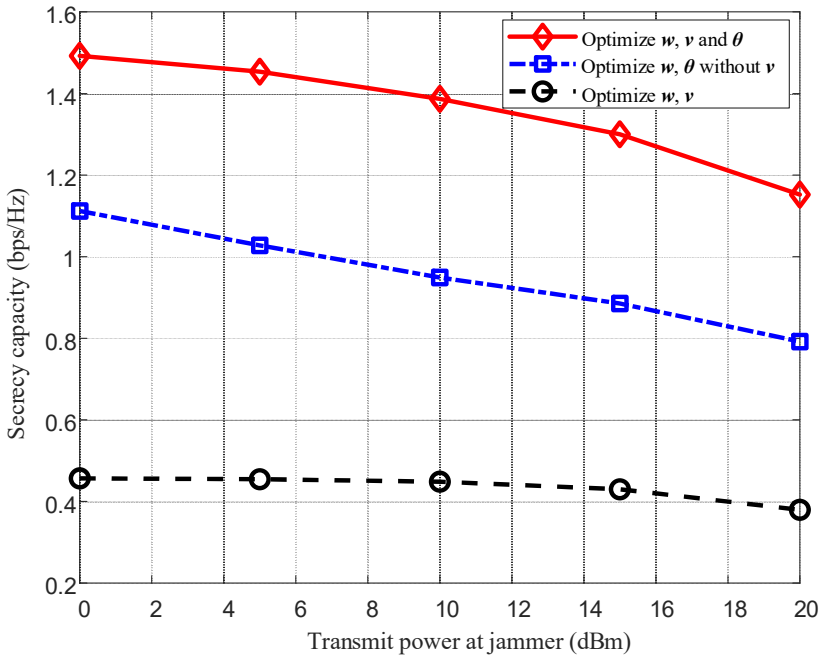

Fig. S1 Secrecy capacity comparison versus transmit power P_{J} for different baseline schemes with M=8

References

Ben-Tal A, Nemirovski A, 2001. Lectures on modern convex optimization: analysis, algorithms, and engineering applications. SIAM.

Guo HY, Liang YC, Chen J, et al., 2020. Weighted sum-rate maximization for reconfigurable intelligent surface aided wireless networks. *IEEE Trans Wirel Commun*, 19(5):3064-3076.